Numerical Study on Tides in the Taiwan Strait and its Adjacent Areas

ZHU Jia[1, 2], HU Jian-yu[1, 2*], ZHANG Wen-zhou[2], ZENG Gan-ning[2,3], CHEN De-wen[1], CHEN Jin-quan[1], SHANG Shao-ping[1]

1. *Department of Oceanography, Xiamen University, Xiamen* 361005*, Fujian Province, China;*

2. *State Key Laboratory of Marine Environmental Science (Xiamen University), Xiamen* 361005*, Fujian Province, China;*

3. *Marine Technology, Zhejiang University of Technology, Hangzhou 310014, Zhejiang Province, China*

Abstract: Diurnal and semi-diurnal tides in the Taiwan Strait and its adjacent areas are calculated by using a two-dimensional finite-difference model. Compared with data of more than 20 observation stations around the Taiwan Strait, the model-produced results agree quite well with those of previous researches using observational data from coastal tidal gauge stations. According to the results, the co-tidal and co-range charts are given. Furthermore, the characteristics of 8 major tidal constituents have been illuminated respectively. The result shows that: (1) The tide motion can be attributed to the interaction between the degenerative rotary tidal system in the north and the progressive tidal system in the south. (2) The southward and northward tidal waves of semi-diurnal tide converge in the middle of the Taiwan Strait while the diurnal tidal waves propagate southwestward through the Taiwan Strait and the Luzon Strait. (3) The maximum amplitude of semi-diurnal tides exists at the area between the Meizhou Bay and Xinghua Bay, and that of diurnal tides appears in the region to the east of the Leizhou Peninsula. (4) The patterns of co-tidal and co-range charts of N_2, K_2 and P_1, Q_1 tidal constituents are similar to those of M_2, S_2 and K_1, O_1 tidal constituents, respectively.

Keywords: Taiwan Strait and its adjacent areas, tidal characteristics, model

The type of the tides from the Pacific Ocean becomes more complex when the tidal wave enters the research region, Taiwan Strait and its adjacent areas, affected by the complex bottom topography, devious coastal boundary, continental shelf and Taiwan Island.

Several kinds of studies on tides in the Taiwan Strait and its adjacent areas have been conducted these years, including four study methods: the analysis of historic data, numerical modeling, the analysis of satellite data, and the assimilation of numerical modeling result with satellite data. On the basis of the tidal data cited from *the tide table of British Navy* and the historic data from the domestic and overseas tidal observation station, several scholars analyzed the basic features of tides and tidal currents in the South China Sea and the Taiwan Strait (e.g. Zheng et al., 1982; Ding, 1983; Yu et al., 1984; Liu et al., 2002). Ye et al (1985), Ye and Ye (1986), Ye (1990) and Yan and Wu (1995) studied the semi-diurnal and

Received on March 13, 2008

*Corresponding author: hujy@xmu.edu.cn

diurnal tides in the Taiwan Strait. Fang et al. (1985, 1986, 1994) established two models with the resolution of 10 nm×10 nm and 0.25° × 0.25° for the M_2, K_1, O_1 tidal constituents of the Taiwan Strait and for the m_1, M_2 tidal constituents of the South China Sea, respectively, and then presented the tidal charts of M_2, K_1 tidal constituents in the studied area. Cao et al. (1990) simulated the semi-diurnal and diurnal tidal constituents in the northern part of the South China Sea. Zhao et al. (1995) calculated four major tidal constituents in the South China Sea with the resolution of 1° × 1° and 30′ × 30′, respectively. Qian et al. (2000) draw the tidal charts of nine tidal constituents in the East China Sea. Jan et al. (2004) developed a three-dimensional model for current and tide in the Taiwan Strait with the resolution 3 km × 3 km. Sha et al. (2000, 2001, 2002) studied the diurnal and semi-diurnal tides around Taiwan by using the Princeton Ocean Model (POM), and then Yu et al. (2003) studied the effect of the tide character by the sea level changes, using the same model, POM. On the other hand, scientists also applied the satellite data for the tide study. Li et al. (2002) analyzed the TOPEX/POSEIDON (T/P) data to get the characters of the four main tidal constituents around Fujian and Taiwan. Hu et al. (2001) and Fang et al. (2004) obtained a large-scale tidal chart in the China Seas and its adjacent sea area by using the 6-years and 10-years T/P data, respectively. Wu et al. (2003, 2004) optimized the boundary condition and the bottom friction coefficient synchronously and simulated the m_1, M_2, S_2, K_1, O_1 tidal constituents in the SCS, assimilated with T/P data and considered the tidal force. Besides, Lin et al. (2001) studied the abnormal amplitude increasing phenomenon of the semi-diurnal tide along the west coast of Taiwan from theoretic and model aspects. Jan et al. (2004) discussed the mechanism of the abnormal amplitude increasing of the M_2 tidal constituent in the Taiwan Strait, and pointed out that the main reason was the coexistence of the progressive wave in the west and the standing wave in the east of strait. Zeng et al. (2004) summarized the research results of M_2 tidal constituent in the Taiwan Strait in recent years.

Taiwan Strait is the channel between the northern SCS and the southern East China Sea, and the tide motion can be attributed to the interaction of the tidal systems both from the north and the south. We consider the Taiwan Strait and its adjacent areas as an entire region and simulate 8 major tidal constituents using a two-dimensional finite-difference model. Then the tidal features for 8 major tidal constituents can be drawn with the 6′×6′ resolution according to the simulation results.

1 Brief introduction of the model

1.1 Model domain

The computational region of this model covers 110 °E - 130°E, 18 °N - 30°N, including the Taiwan Strait, the southern East China Sea, the deep water area east of Taiwan Island, and the Luzon Strait. The model domain is shown in Fig. 1, demonstrating that the water depth is up to one thousand meters offshore the eastern Taiwan Island, decreases westward to tens of meters in the Taiwan Strait, and increases as deep as thousands meters in the southern deep sea of the Taiwan Bank. The tide motion becomes complex because of the rough bottom topography.

1.2 Model equation

$$\frac{\partial \zeta}{\partial t}+\frac{\partial Hu}{\partial x}+\frac{\partial Hv}{\partial y}=0 \tag{1}$$

$$\frac{\partial u}{\partial t}+u\frac{\partial u}{\partial x}+v\frac{\partial u}{\partial y}-fv=-g\frac{\partial \zeta}{\partial x}-\frac{\tau_{bx}}{\rho H} \tag{2}$$

$$\frac{\partial v}{\partial t}+u\frac{\partial v}{\partial x}+v\frac{\partial v}{\partial y}+fu=-g\frac{\partial \zeta}{\partial y}-\frac{\tau_{by}}{\rho H} \tag{3}$$

where x, y are the horizontal axises of Descartes, which is positive eastward, northward, and upward respectively for x, y and z axis; t stands for time; u, v for average mean velocity in x, y direction respectively:

$$u=\frac{1}{H}\int_{-h}^{\zeta}u'dz\,;\quad v=\frac{1}{H}\int_{-h}^{\zeta}v'dz \tag{4}$$

here, ζ stands for the water level calculated from the undisturbed sea surface; $H=\zeta+h$, is the height of the water column, h is water depth; g is the acceleration of gravity; f is the Coriolis parameter, $f=2\Omega\sin\varphi$, φ stands for the latitude, $\Omega=7.29\times10^{-5}/s$. In this model, the bottom friction is:

$$\tau_b=\rho g C^{-2}\left|\vec{U}\right|\vec{U}\,,\qquad C=\frac{1}{n}h^{\frac{1}{6}} \tag{5}$$

here n is the Manning coefficient, n=0.03; ρ is the density of seawater; $\vec{U}$ is the velocity of the vertical flow; C is the bottom drag coefficient.

1.3 Initial and boundary condition

The model begins running with the initial condition, that is, $\zeta=u=v=0$. We suppose the boundary is a zigzag line, and goes through u and v points, $u=0$ or $v=0$. In another word, we make the value of the average vertical velocity in normal direction to be zero. sFinally, we consider the entire water boundary as being forced by the water level:

$$\zeta_i=H_i\cos(\sigma_i t+v_{0i}-g_i)\qquad (i=1,2,3.....8) \tag{6}$$

In this formula, H_i is the amplitude of the tidal constituent i, g_i is its phase, σ_i is the angular velocity; and v_{0i} is the astronomical initial phase, which can be calculated through the formulae (Fang et al., 1986) of astronomical basic factor.

In this model, we adopt an implicit difference method, second-order accurate and unconditionally stable, staggered grid (C grid), with the resolution 6′×6′ in this research region. It can be divided into

201×121 grid points, and the distance between each grid point is about 11 km. The water depth of each grid point is the average depth of that gird. The time step is set to be 200 s.

This research region includes a long opening boundary. How to get the appropriate value of the forcing boundary is a key step in the numerical calculation of astronomical tide. In our model, we adopt a global model's result, NAOTIDE, whose resolution is 0.5° × 0.5°. We input the interpolated result as the boundary condition, and then slightly adjust the boundary value through a series of numerical experiments. After the model calculation being stable, we output one month of water level value, with one hour interval, then analyze the harmonic constants with the Least Square Method (Fang et al., 1986), and finally draw the co-tidal charts of the eight major tidal constituents for analyzing the character of each tide.

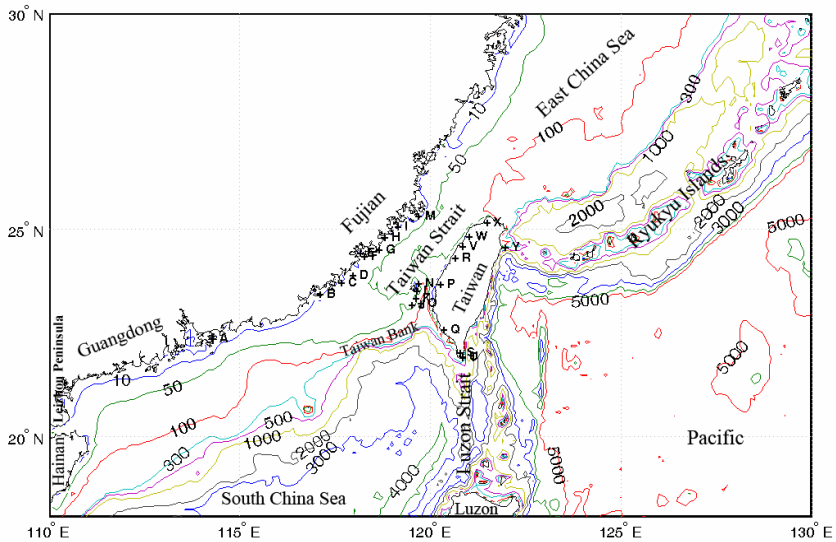

Fig. 1 Topography of the model domain

(A-ShenZhen, B-NanAo, C-DongShan, D-FuTou Bay, E-XiaMen, F-JinMen, G-WeiTou, H-QuanZhou, I-Meizhou, J-Xiji Island, K-Jiangjun'ao, L-Magong, M-Xinghua Bay, N-Baisha Island, O-Dongji, P-Kouhu, Q-Gaoxiong, R-Taizhong, S-Checheng, T-Houbi Lake, U-Dabanlie, V-Houlong, W-Xinzhu, X-Danshui, Y-Su'ao)

2 Comparison between calculated result and observed data

In the validation process, we compare the calculated result with the observation derived harmonic constants which extracted from the book named *Tide application along China coast* written by Wang (1986) (the data were from Royal Navy tide table, reports of Japanese waterway department and publication of the USSR etc.). The comparison of four major tidal constituents (M_2, S_2, K_1, O_1) is shown in Tab. 1.

The comparison result shows: the average absolute deviations of amplitude and phase for M_2 tidal constituent are 4.1 cm and 5.6°, respectively. The absolute amplitude deviation ranges from 0.5 cm to 3 cm; the minimum absolute deviation of amplitude is 0.1 cm at Station Dabanlie, and the maximum is

16.4 cm at Station Xiamen because the station's grid point does not match the geographical position. The absolute phase deviation ranges from 0.6 to 5.5°, with the maximum deviation 16.5° at Station Kouhu. The average absolute deviations of amplitude and phase for S_2 tidal constituent are 7.4 cm and 10.5°, respectively. The absolute amplitude deviations of most stations are less than 10 cm, the maximum and minimum deviations are 19.4 cm and 0.6 cm at Station Nan'ao and Danshui respectively; the maximum deviation of phase is 23.5° at Station Jiangjun'ao. The average absolute deviations of amplitude and phase for K_1 and O_1 tidal constituents are 2.3 cm and 6.3°, 3.2 cm and 7.5°, respectively.

For the rest four tidal constituents (P_1, Q_1, N_2, K_2), due to the lack of the harmonic constants from observation data, we compare the model result indirectly. Wang (1986) and Fang et al. (1986) proposed similar empirical formulae to induce the harmonic constants of P_1, Q_1, N_2, K_2 tidal constituents from M_2, S_2, K_1, O_1 tidal constituents. Their empirical formulae are the same for amplitude, but quite different with each other for phase. Here we use the amplitude empirical formulae as equations. (7) - (10) to calculate the harmonic constants of P_1, Q_1, N_2, K_2 tidal constituents through M_2, S_2, K_1, O_1 tidal constituents , then compare with our model results, and finally get the average absolute deviations of each tidal constituent as shown in Tab. 1. The average absolute deviation of amplitude of P_1, Q_1, N_2, K_2 tidal constituents are 1.2 cm, 1.0 cm, 4.5 cm and 5.3 cm, respectively.

$$H_{p_1} = 0.3333 H_{k_1} \qquad g_{p_1} = g_{k_1} - 0.075(g_{k_1} - g_{o_1}) \tag{7}$$

$$H_{Q_1} = 0.2000 H_{o_1} \qquad G_{Q_1} = G_{k_1} - 1.499(g_{k_1} - g_{o_1}) \tag{8}$$

$$H_{N_2} = 0.2000 H_{M_2} \quad g_{N_2} = g_{M_2} \tag{9}$$

$$H_{k_2} = 0.2725 H_{s_2} \qquad g_{k_2} = g_{s_2} - 0.081(g_{s_2} - g_{M_2}) \tag{10}$$

According to the statistics, the model result of M_2 matches the observation data quite well, as well as the results of K_1 and O_1 tidal constituents. The model results of P_1 and Q_1 tides are close to the value induced from the empirical formulae, the distribution patterns also accord with the co-tidal features obtained from the satellite altimeter data; but the model amplitudes of N_2 and K_2 are a little larger than the theoretic value.

3 Co-tidal and co-range charts for each tidal constituent

3.1 M_2 tidal constituent

As shown in Fig. 2a, the amplitude of M_2 tidal constituent is greater nearshore but smaller offshore. The water depth is thousand meters off the east coast of the Taiwan Island so the amplitude there is less than 60 cm. There's a small amplitude area near the northeast cape of Taiwan Island, the amplitude is no more than 40 cm. In the Taiwan Strait, the tidal amplitude zooms as the water depth decreases, especially

at the Taiwan Bank area. This figure also shows that the amplitude in the west coast is larger than that in the east coast, caused by the Coriolis force. Near the Meizhou Bay and the Xinghua Bay, the amplitude is more than 200 cm, and the maximum amplitude (223 cm) appears around the (119.5ºE, 25.2ºN) sea area. At the shelf area of northern South China Sea, the amplitude increases from 20 cm to 80 cm as a result of "shelf effect", and the large amplitude appears close to the west Guangdong Province.

Tab. 1 Comparisons of calculated and observed harmonic constants for each tidal constituent

station	Lon&lat		gridding		Absolute Error / M_2		Absolute Error / S_2		Absolute Error / K_1		Absolute Error / O_1		Amplitude Absolute Error / cm			
	E	N	I	J	H / cm	G / °	H / cm	G / °	H / cm	G / °	H / cm	G / °	P_1	Q_1	N_2	K_2
Shenzhen	114°12′	22°24′	42	44	3.82	5.37	1.18	6.49	0.99	0.77	3.95	7.10	0.57	-1.11	0.19	3.71
Nan'ao	117°01′	23°28′	70	55	12.40	14.98	19.43	19.28	0.93	7.33	1.17	5.13	1.00	-0.10	-7.89	8.71
Dongshan	117°34′	23°45′	76	58	4.43	0.65	18.46	4.99	0.50	6.85	1.50	8.57	1.00	-0.11	-7.22	8.76
Futou Bay	117°52′	23°55′	79	59	7.22	2.04	11.73	1.73	0.19	3.47	4.83	9.77	0.60	-1.30	-3.20	8.54
Xiamen*	118°04′	24°27′	81	64(63)	16.41	0.82	10.18	0.82	4.17	2.80	7.95	11.50	2.20	-2.10	-2.86	8.07
Jinmen	118°10′	24°23′	82	64	2.88	0.81										
Weitou	118°34′	24°32′	86	65	2.17	0.72	14.17	1.08	3.75	2.63	7.59	11.22	2.10	-2.10	-8.10	10.07
Quanzhou*	118°43′	24°49′	87	68(66)	2.94	14.22	7.28	6.19	3.69	0.84	7.53	14.74	2.10	-2.03	-8.69	10.11
Meizhou*	119°03′	25°05′	91	71(70)	0.46	5.30	5.61	17.49	3.72	15.51	4.41	5.24	2.00	-1.40	-12.70	9.98
Xiji Island	119°25′	23°13′	94	52	9.38	7.38										
Jiangjun'ao	119°31′	23°22′	95	54	8.61	4.72	9.85	23.52	2.57	4.52	0.13	6.33	1.60	-0.38	-3.00	5.13
Magong	119°33′	23°33′	95	55	0.07	2.91	2.50	17.16	0.03	6.56	0.09	5.03	0.70	-0.40	-5.28	2.96
Xinghua Bay	119°35′	25°20′	96	73	1.25	7.13	4.08	17.75	3.68	16.33	4.15	4.63	2.00	-1.41	-16.60	7.04
Baisha Island*	119°36′	23°44′	96	56(57)	5.69	1.04	0.66	0.28	2.71	8.87	0.11	7.10	1.60	-0.38	0.60	3.33
Dongji	119°40′	23°15′	97	53	0.74	2.52										
Mazu	119°55′	26°10′	99	82			11.85	11.28	1.02	3.76	2.05	2.76	0.40	-0.95	-6.97	2.47
Kouhu	120°10′	23°42′	102	57	0.83	16.48	8.91	1.58	4.69	7.55	5.19	8.51	2.20	-1.50	-7.08	6.76
Gaoxiong	120°16′	22°37′	103	46	7.15	7.50	2.45	22.44	4.54	17.94	3.95	14.71	2.17	-1.20	0.60	-0.24
Taizhong	120°33′	24°20′	105	63	0.20	1.91										
Checheng	120°41′	22°04′	107	41	2.03	5.48	4.75	14.28	1.43	10.30	1.94	6.17	0.27	-0.90	1.69	-0.63
Houbi Lake	120°45′	21°57′	108	39	2.18	10.96										
Dabanlie	120°45′	21°58′	108	40	0.06	9.25	4.55	9.08	2.42	1.96	0.82	10.01	0.03	-0.80	1.84	-0.10
Houlong*	120°45′	24°37′	108	67(66)	8.89	5.11	1.16	13.38	2.86	0.46	2.12	3.92	1.60	-0.97	-13.60	7.95
Xinzhu	120°55′	24°51′	109	69	0.78	1.44										
Danshui*	121°24′	25°11′	114	73(72)	1.06	4.54	0.57	12.14	0.21	4.63	0.74	1.68	0.50	-0.48	4.62	2.63
Su'ao*	121°52′	24°35′	119	65(66)	1.41	5.53	7.67	8.28	1.16	2.27	3.80	6.06	0.20	0.11	3.73	-0.31
Average					4.1	5.6	7.4	10.5	2.3	6.3	3.2	7.5	1.2	1.0	4.5	5.3

remark：'*' stands for the station whose location does not match the real observation station, using the closest gridding point instead.

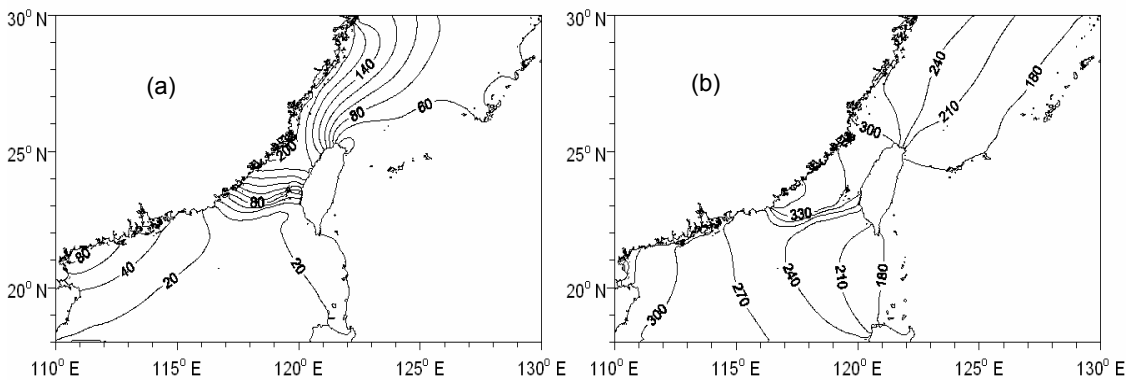

Fig. 2 Co-tidal and co-range charts of M_2 tidal constituent

(a) amplitude (cm); (b) phase (°) referred to 120°E.

Fig. 2b indicates that the co-range lines distribute sparsely to the east of the Taiwan Island, suggesting the tidal waves propagate quickly in deep water. In the southern sea area of the Taiwan Island, the co-range lines distribute evenly, and the tidal waves propagate westward from the Luzon Strait to the east coast of the Hainan Island. In the northern area of Taiwan Island, the co-range lines rotate anticlockwise around the north cape of the Taiwan Island, with the phase increasing from 180° to 300°, so as to become a degenerative rotary tidal system (Shen, 1980). As the north and south tidal waves meet around the Taiwan Bank, the distribution of the co-range lines becomes denser as the water depth being shallower.

Obviously, the amplitude of M_2 tidal constituent is large in the west but small in the east, while large in the north but small in the south of Taiwan Strait. The amplitude increases as the south and north tidal waves meet in the middle of the Taiwan Strait, and reach the maximum near the Meizhou Bay-Xinghua Bay of Fujian Province. The time of high tide defers gradually from south or north to the middle part of the Taiwan Strait, and the latest high tide place is near Dongshan, Fujian Province.

Compared with the other research results, the distribution pattern of the co-tidal and co-range lines are accordant with the results of Fang et al. (1985) and Sha et al. (2000). The maximal amplitude appears near the Meizhou Bay-Xinghua Bay, which is also the same as that from previous results. In this model, the maximal amplitude is 223 cm, close to the result of Fang et al. (1985) and Sha et al. (2000), whose maximal amplitude is 200 cm and 240 cm, respectively. However, there still exist some divarications about the influence range and strength of north and south tidal waves in the Taiwan Strait. Some scholars considered that the north tidal wave is dominant and can spread to the Taiwan Bank, but some others insisted that the south tidal wave is stronger than ever understood, and the influence range is farther into the northern part of the Taiwan Strait. But the influence range of the two tidal waves cannot be distinguished directly; it will be discussed with further consideration of the tidal current distributions.

3.2 S_2 tidal constituent

S_2 tidal constituent is also a semi-diurnal tide, so its patterns of the amplitude and phase (Fig. 3) are similar to those of the M_2 tidal constituent. The amplitude of S_2 ranges from 10 cm to 20 cm in the east area of the Taiwan Island. There is a small amplitude area near the north cape of the Taiwan Island, for the amplitude there is smaller than 10 cm. The amplitude is higher than 30cm in the Taiwan Strait, and the maximum amplitude (80 cm) appears around the Xinghua Bay, almost the same as that of M_2 tidal constituent.

The co-range lines rotate anticlockwise around the north cape of the Taiwan Island, with the phase increasing from 210° to 360°, and become a degenerative rotary tidal system there (Shen, 1980), which is more obvious than that in M_2 tidal constituent. There exists an amphidromic point in the southwest of Taiwan Island, but such an amphidromic point was not mentioned by Ye et al. (1985), Wu et al.(2004) and Sha et al. (2001) (see Fig. 4a) . However, the present model result is similar with that of Hu et al. (2001), which inferred from the T/P altimeter data that there are two obvious amphidromic points near the Taiwan Bank (Fig. 4b).

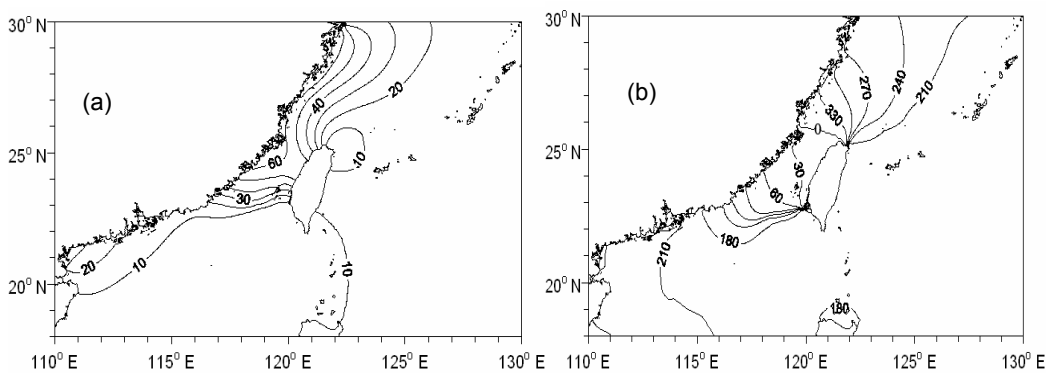

Fig. 3 Co-tidal and co-range charts of S_2 tidal constituent

(a) amplitude (cm); (b) phase (°) referred to 120°E

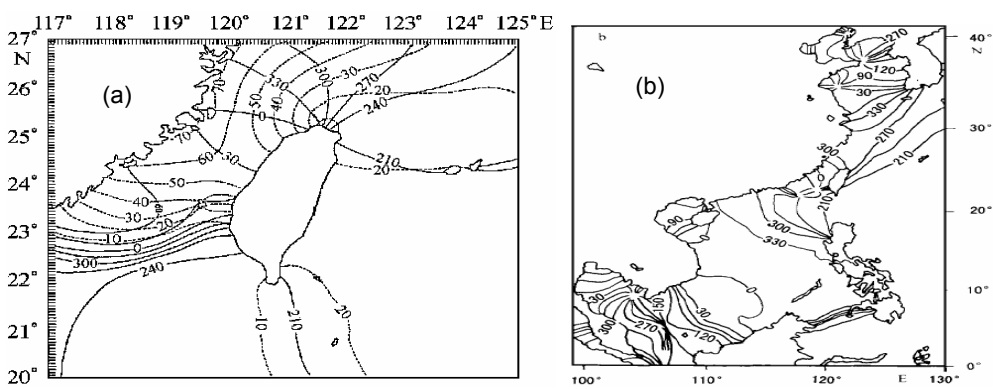

Fig. 4 Co-tidal and co-range charts of S_2 tidal constituent in the Taiwan Strait.

(a) cited from Sha et al. (2001); (b) cited from Hu et al. (2001)

3.3 K_1 and O_1 tidal constituents

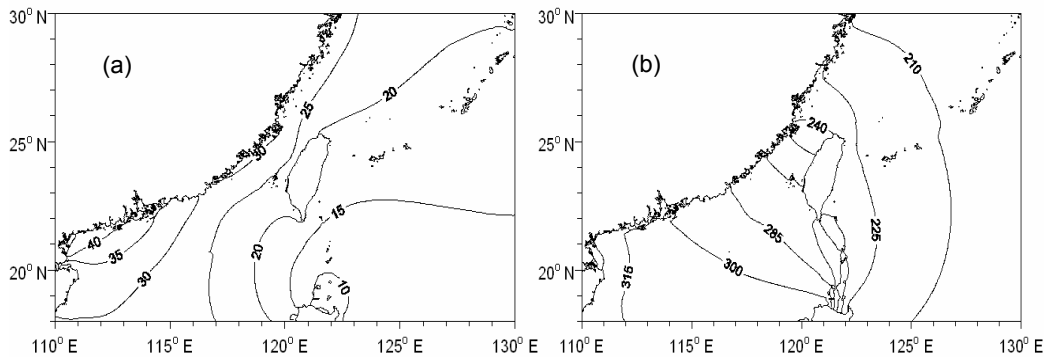

Fig. 5 Co-tidal and co-range charts of K_1 tidal constituent

(a) amplitude (cm); (b) phase (°) referred to 120°E

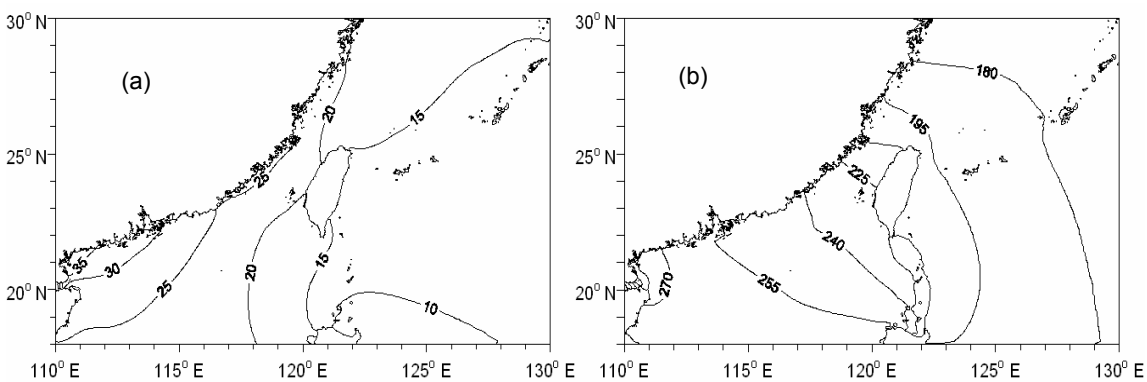

Fig. 6 Co-tidal and co-range charts of O_1 tidal constituent

(a) amplitude (cm); (b) phase (°) referred to 120°E

It can be seen from Fig. 5a that the co-tidal lines of K_1 tidal constituent distribute evenly in the studied area. The amplitude increases gradually from north to south and from east to west. The co-tidal lines are almost parallel to the coastline in the Taiwan Strait, and the amplitude is no less than 30 cm in the western part while it is 20 - 25 cm in the eastern part. The large amplitude area appears between the Qiongzhou Strait and the eastern Leizhou Peninsula, with the maximum amplitude of 45 cm.

The co-range lines of K_1 tidal constituent are about perpendicular to the co-tidal lines in the Taiwan Strait, and distribute densely in the Luzon Strait, with the phase ranging from 225° to 300°. In the Taiwan Strait, the high tide time in the west coast is later than that in the east coast at the same latitude, that is, the high tide time defers slightly from east to west. According to the distribution pattern, the propagating path of K_1 tidal constituent can be deduced: after the tidal wave entering the studied area from the west Pacific, it propagates southwestward through the Taiwan Strait and the Luzon Strait.

As the Fig. 6 shown, the distribution pattern of O_1 tidal constituent is similar to K_1, no matter the

amplitude or the phase. The amplitude of O_1 tidal constituent is 5 cm - 10 cm smaller than that of K_1, and the maximum amplitude (45 cm) appears in the Qiongzhou Strait. The propagating direction is also southwestward, the same as K_1 tidal constituent, so the high tide time defers slightly from east to west too, and the high time appears near the Leizhou Peninsula and the Qiongzhou Strait. But the phase of O_1 tidal constituent is 20º ahead to that of K_1 tidal constituent.

As compared with M_2 and S_2 tidal constituents, the amplitude maximum of K_1 and O_1 tidal constituents appear near the Leizhou Peninsula and the Qiongzhou Strait in stead of the middle Taiwan Strait. Furthermore, the co-tidal and co-range lines of K_1 and O_1 tidal constituents do not distribute densely around the Taiwan Bank, indicating that the diurnal tidal waves directly enter the SCS through the Taiwan Strait and the Luzon Strait. This is due to that the diurnal tidal waves dissipate less energy than the semi-diurnal tidal waves (Ye and Ye, 1986), so it can accumulate enough energy to propagate through the Taiwan Strait from northeast to southwest.

3.4 P_1 and Q_1 tidal constituents

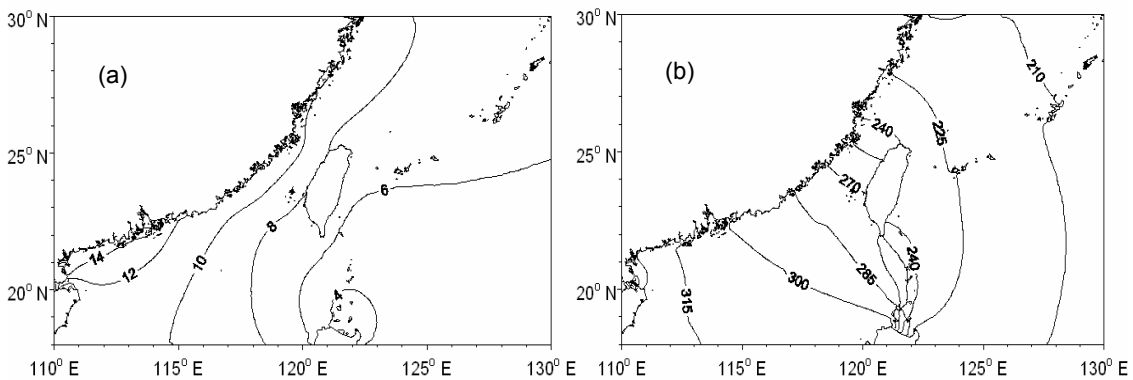

Fig. 7 Co-tidal and co-range charts of P_1 tidal constituent

(a) amplitude (cm); (b) phase (°) referred to 120°E

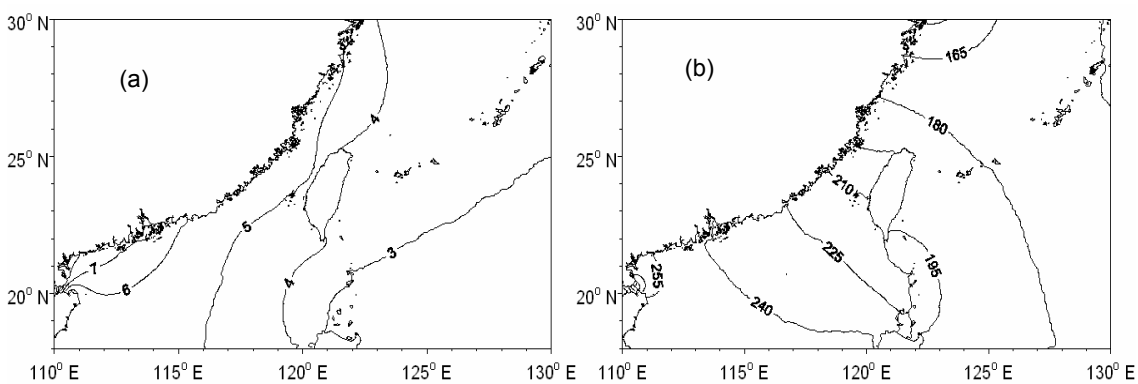

Fig. 8 Co-tidal and co-range charts of Q_1 tidal constituent

(a) amplitude (cm); (b) phase (°) referred to 120°E

As demonstrated in Fig. 7 and Fig. 8, the distribution patterns of co-tidal and co-range of P_1 and Q_1 are quite similar to those of the other major diurnal tidal constituents. The co-tidal lines are perpendicular to the co-range lines, and the phase value increases from northeast to southwest. The maximal amplitudes of P_1 and Q_1 tidal constituents are no more than 15 cm, ranging from 3 cm - 15 cm for P_1 tidal constituent and 3 cm - 8 cm for Q_1 tidal constituent, respectively. The phase of P_1 tidal constituent is close to that of K_1, increasing southwestward from 210° to 330°, while the phase of Q_1 tidal constituent is close to that of O_1, ranging from 170° to 260°. The tidal wave propagates faster in the Luzon Strait, densely in the phase lines there. The maximal amplitude appears almost in the same area, nearshore the eastern Leizhou Peninsula, for both P_1 and Q_1 tidal constituents.

3.5 N_2 and K_2 tidal constituents

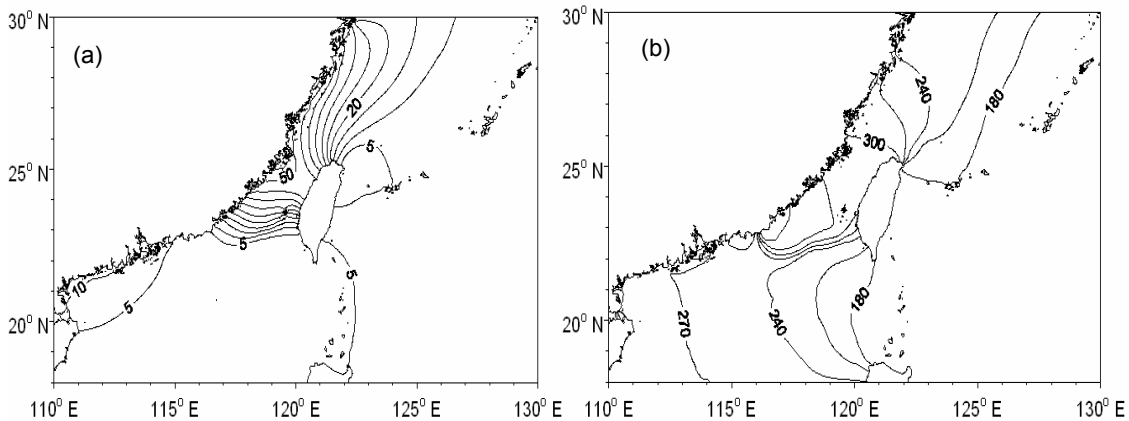

Fig. 9 Co-tidal and co-range charts of N_2 tidal constituent

(a) amplitude (cm); (b) phase (°) referred to 120°E

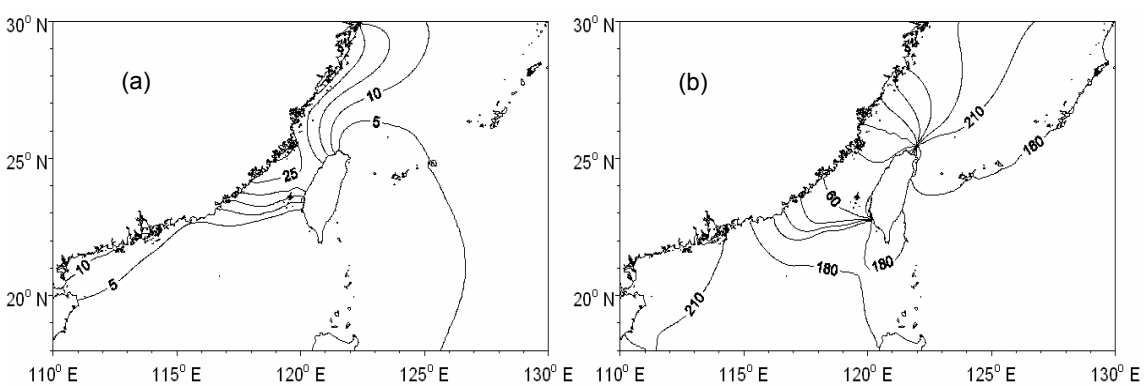

Fig. 10 Co-tidal and co-range charts of K_2 tidal constituent

(a) amplitude (cm); (b) phase (°) referred to 120°E

N_2 and K_2 tidal constituents are similar with M_2 and S_2 tidal constituents, respectively, no matter the amplitude pattern or the phase pattern. The amplitude in the west is larger than that in the east of the strait.

The co-range distribution also shows that a degenerative rotary tidal system exists near the north cape of Taiwan Island. The amplitude increases as the south and north tidal waves converge in the Taiwan Strait. The phase patterns of N_2 and K_2 tidal constituents are almost consistent with those of M_2 and S_2 tidal constituents, respectively.

4 Conclusions

The harmonic constants of 8 principal tidal constituents have been calculated and validated, and the co-tidal features are given in this paper. The main conclusions include:

(a) It is indicated from the comparisons that the model result matches basically with the observation one. The average absolute deviations for amplitude of four tidal constituents, M_2, S_2, K_1 and O_1, are 4.1 cm, 7.4 cm, 2.3 cm and 3.2 cm respectively; and the average absolute deviations for the phase of these tidal constituents are 5.6°, 10.5°, 6.3°and 7.5°, respectively. The average absolute deviations of amplitude for P_1, Q_1, N_2 and K_2 tidal constituents are 1.2 cm, 1.0 cm, 4.5 cm and 5.3 cm, respectively.

(b) In the model domain, the tide propagates from the western Pacific. The semi-diurnal tide consists of two branches, which enter the Taiwan Strait from south and north respectively. The north branch is a degenerative rotary tidal system, and converges with the south branch in the middle of Taiwan Strait. The diurnal tide obviously takes the Kelvin wave form when it propagates through the Taiwan Strait.

(c) The maximal amplitude of the semi-diurnal tides appears around the Meizhou Bay and Xinghua Bay, Fujian Province. The maximum values of M_2 and S_2 are 223 cm and 80cm respectively. The maximal amplitude of the diurnal tides appears near the Qiongzhou Strait and the Leizhou Peninsula, with the maximum amplitude of about 40 cm.

(d) For S_2 tidal constituent, there is an obvious amphidromic point near the Taiwan Bank.

(e) The patterns of co-tidal and co-range charts of N_2, K_2 and P_1, Q_1 are similar to those of M_2, S_2 and K_1, O_1, respectively.

Acknowledgements

This research is jointly supported by the National Natural Science Foundation of China under contract Nos. 40576015, 40810069004 and 40821063, by the key research project of Fujian Province under contract No. 2004N203, and by the Fujian demonstrating region of the “863” Project of the Ministry of Science and Technology of China.

Reference

[1] Cao M D, Fang G H. A numerical model for tides and tidal currents in northern South China Sea [J]. Tropic

Oceanology, 1990, 9(2): 63-70.

[2] Ding W L. The characteristics of the tides and tidal currents in the Taiwan Strait [J]. Journal of Oceanography in Taiwan Strait, 1983, 2(1): 1-8.

[3] Fang G H, Yang J F, Zhao X C. A numerical model for tides and tidal currents in Taiwan Strait [J]. Acta Oceanologica Sinica, 1985, 7(1): 12-21.

[4] Fang G H. Tide and tidal current charts for the marginal seas adjacent to China [J]. C. J. of Oceanology and Limnology, 1986, 4(1): 1-16.

[5] Fang G H, Cao M D, Huang Q Z. A numerical model of tides and tidal currents in South China Sea [J]. Acta Oceanologica Sinica, 1994, 16(4): 1-12.

[6] Fang G H, Wang Y G, Wei Z X, et al. Empirical cotidal charts of the Bohai, Yellow and East China Seas from 10 years of TOPEX/Poseidon altimetry [J]. Journal of Geophysical Research, 2004, 109: 1-13.

[7] Fang G H, Zheng W Z, Chen Z Y, et al. Analysis and forecast of tides and tidal currents. Beijing: Beijing Press, 1986.

[8] Hu J Y, Kawamura H, Hong H S, et al. Tidal features in the china seas and their adjacent sea areas as derived from TOPEX/POSEIDON altimeter data [J]. Chinese Journal of Oceanology and Limnology, 2001, 19(4): 293-305.

[9] Jan S, Wang Y H, Wang D P, et al. Incremental inference of boundary forcing for a three-dimensional tidal model: tides in the Taiwan Strait [J]. Continental Shelf Research, 2004, 24: 337-351.

[10] Jan S, Chen C S, Wang J, et al. The anomalous amplification of M_2 tide in the Taiwan Strait [J]. Geophysical Research Letters, 2004, 31: 1-4.

[11] Lin M C, Juang W J, Tsay T K. Anomalous amplifications of semidiurnal tides along the western coast of Taiwan [J]. Ocean Engineering, 2001, 28: 1 171-1 189.

[12] Liu J F, Liu Z, Gu Y Y, et al. Analysis of the hydrographic elements features in Taiwan Strait [J]. Marine Forecasts, 2002, 19(3): 22-32.

[13] Li Y C, Cai W L, Li L, et al. The tide characteristics of the seas adjacent to Fujian and Taiwan derived from TOPEX/POSEIDON altimeter data [J]. Acta Oceanologica Sinica, 2002, 24(supplement 1): 154-162.

[14] Qian C C, Shen Y.J. Distribution of 9 principal tidal constituents and tide prediction for the East China Sea [J]. China Ocean Engineering, 2000, 14(4): 541-548.

[15] Sha W Y, Lu X G, Jiang G R. Numerical simulation of M_2 tide characteristics in the sea area around Taiwan Strait Island [J]. Journal of PLA University of Science and Technology. 2000, 1(1): 80-87.

[16] Sha W Y, Lu X G, Chen X, et al. Numerical simulation of characteristics of semidiurnal tidal waves in sea region around Taiwan [J]. Acta Oceanologica Sinica, 2001, 23(4): 31-40.

[17] Sha W Y, Lu X G, Zhang W J, et al. Synthetic property of diurnal constituent, tide and tidal current of the sea regions around Taiwan Island [J]. Marine Science, 2002, 26(10): 62-69.

[18] Shen Y J. Numerical computation of tides in the East China Sea [J]. Journal of Shangdong College of Oceanology, 980, 10(3): 26-35.

[19] Wu Z K, Tian J W, Lu X Q, et al. A numerical model of tides in the South China Sea by adjoint method [J]. Oceanologia et limnologia sinica, 2003, 34(1): 101-108.

[20] Wu Z K, Tian J W, Zhao Q. 3-D numerical simulation of the South China Sea tidal waves with assimilation

method [J]. Journal of Hydrodynamics, 2004, 19(4): 501-506.

[21] Wang Z H. Tide application along China coast. 1986.

[22] Yan T Z, Wu Y C. Numerical study on upwelling along Fujian coast I. numerical modeling on tide and tidal current in the Taiwan Strait [J]. Studia Masina Sinica, 1995, 36: 47-53.

[23] Ye A L, Chen Z Y, Yu Y F. Numerical investigation of three-dimensional semi-diurnal tidal waves in Taiwan Strait and its adjacent areas [J]. Oceanologia et Limnologia Sinica, 1985, 16(6): 439-450.

[24] Ye A L, Ye J H. Numerical investigation of three-dimensional diurnal tidal waves in Taiwan Strait and its adjacent areas [J]. Oceanologia et limnologia Sinica, 1986, 17(3): 260-265.

[25] Ye A L. Kelvin wave in Taiwan Strait [J]. Marine Science Bulletin, 1990, 9(5): 1-5.

[26] Yu G M. The basic analysis of the tidal characteristics in the South China Sea [J]. Acta Oceanologica Sinica, 1984, 6(3): 293-300.

[27] Yu Y F, Yu Y X, Zuo J C, et al. Effectof sea level variation on tidal characteristic value for the East China Sea [J]. China Ocean Engineering, 2003, 17(3): 369-382.

[28] Zeng G N, Qi Y Q, Hu J Y, et al. Advances in the M_2 tide wave research in the Taiwan Strait [J]. Advances in Marine Science, 2004, 22(4): 508-518.

[29] Zhao M C, Han X H. The calculation and research for the tidal charts in the China seas [J]. Advances in Water Science, 1995, 1: 23-30.

[30] Zhen W Z, Chen F N, Chen X Z. The tides and tidal currents in the Taiwan Strait [J]. Journal of Oceanography in Taiwan Strait, 1982, 1(2): 1-4.

台湾海峡及其邻近海域潮汐数值计算

朱 佳[1,2]，胡建宇[1,2]，张文舟[2]，曾淦宁[2,3]，陈德文[1]，陈金泉[1]，商少平[1]

（1．厦门大学海洋学系 亚热带海洋研究所，福建 厦门 361005；2. 厦门大学 近海海洋环境科学国家重点实验室，福建 厦门 361005；3．浙江工业大学海洋技术专业，杭州 浙江 310014）

摘 要：建立二维潮波模式，模拟了台湾海峡及其邻近海域(18 ～ 30°N，110 ～ 130°E)八个主要分潮(M_2、S_2、K_1、O_1、P_1、Q_1、K_2、N_2)，并利用中国大陆及环台湾岛20多个潮位站的实测资料进行验证，计算结果与实测值吻合良好。此外，给出了八个主要分潮的同潮图，并逐个讨论了潮汐特征。结果显示：(1) 台湾海峡中的潮波运动是北部蜕化了的旋转潮波系统和南部的前进潮波系统共同作用的结果。(2) 半日分潮南、北两支潮波在台湾海峡中部汇合，而全日分潮则在台湾海峡南部海域汇合后继续朝西南方向传播。(3) 半日分潮振幅最高值发生在福建省湄洲湾—兴化湾一带，全日分潮最高值则出现在雷州半岛以东一带近岸海域。(4) N_2、K_2 和 O_1、P_1、Q_1 分潮的振幅、迟角分布分别同 M_2 与 K_1分潮的整体分布趋势相似。

关键词：物理海洋学；台湾海峡及其邻近海域；潮汐特征；数值计算